MODE I AND MIXED-MODE I/II CRACK TIP FIELDS UNIFIED BY CONSTRAINT

Bostjan Bezensek[1] and John W. Hancock[2]

[1]Faculty of Mechanical Engineering, University of Maribor, Smetanova 17, 2000 Maribor, Slovenia
[2]Department of Mechanical Engineering, University of Glasgow, Glasgow G12 8QQ, Scotland

bostjan.bezensek@uni-mb.si, j.hancock@eng.gla.ac.uk

Abstract

A procedure has been developed to unify cleavage toughness data in mode I and mixed-mode I/II loading into one consistent scheme. Mode I and mixed-mode I/II crack tip fields are shown to belong to the same family of fields, which are deviatorically similar and differ mainly hydrostatically in the leading sectors around the plane of maximum principal stress. This observation allows the unconstrained mode I toughness data to be related to the toughness under mixed-mode conditions for stress controlled cleavage. The procedure is verified with brittle fracture experiments on a plain carbon manganese steel at -90 ^{o}C.

Introduction

Fracture toughness data are usually derived from standard test procedures which are largely concerned with mode I toughness. Mode I loading is particularly significant because it often gives rise to low values of fracture toughness. However in order to demonstrate safety margins the toughness for mixed-mode loading may also be required by defect assessment procedures. Mixed-mode test are more difficult to perform and interpret as discussed by Smith [1]. In the present work a two parameter fracture mechanics procedure is developed that allows mixed-mode crack tip fields to be correlated with the mode I fields by invoking constraint arguments. This procedure allows the toughness under mode I – mixed-mode I/II loading to be unified into one consistent scheme using constraint arguments. This alleviates difficulties associated with mixed-mode I/II testing and provides a basis for unified defect assessment schemes.

Two parameter fracture mechanics [2,3] characterise the crack tip fields with a parameter, such as J, which describes the amplitude of the dominant singularity and a higher order term, such as Q or T which quantify the level of constraint. The assumption that plasticity completely encompasses the crack tip leads to a unique non-trivial field which was originally discussed by Prandtl [4] and is shown in Figure 1a. This highly constrained field is uniquely characterised by J. However Du and Hancock [5] showed that this field is not unique, but the limiting example of a family of fields which depend on the non-singular T-stress. When T is compressive ($T/\sigma_o < 0$) elastic wedges appear on the crack flanks and constraint is lost in the constant stress sector ahead of the crack as shown in Figure 1b. Increasingly negative values of T cause the angular span of the centred fan to decrease, paralleling the forward rotation of the lobes of the plastic zone, accompanied by a loss of constraint in the diamond ahead of the crack. In non-hardening plasticity, changes of the stress state in the leading sector ahead of the crack can only arise from changes in the mean stress. Following O'Dowd and Shih [3] this can be described by the introduction of a constraint parameter, Q*:*

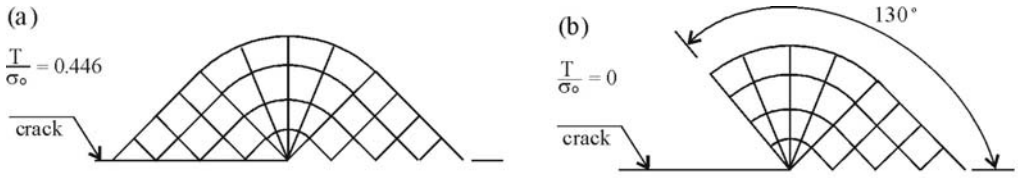

FIGURE 1. Prandtl and T=0 Mode I slip line fields.

$$\sigma_{\theta\theta} = \sigma_{SSY} + Q\sigma_o \quad (1)$$

where σ_{SSY} is the small scale yielding solution and σ_o is the yield stress. O'Dowd and Shih [3] have argued that even in the presence of hardening, Q is largely hydrostatic in nature, leading to a family of fields which are deviatorically similar but hydrostatically different in the leading sectors.

The nature of plane strain mixed-mode fields under elastic-perfectly-plastic conditions has been addressed computationally by Karstensen [6] and Li and Hancock [7]. The mixed mode fields can be usefully regarded as distortion of the Mode I field corresponding to a rotation of the leading constant stress sector, as shown in Figure 2. This allows a continuous plastic field to extend to the crack flanks with a uniform stress triangle on the tensile side, while the elastic wedge on the compressive flank increases its angular span. This process continues with increasing mixity eventually recovering the near mode II fields discussed by Shih [8] and the pure Mode II field proposed by Hutchinson [9]. Zhu and Chao [10] have suggested modifications to the near mode I fields in which the elastic sector is decomposed into an elastic sector plus a small constant stress sector. However as soon as plasticity completes to one crack flank the stresses in the leading constant stress sector are determined only by the mixity of the remote loading. Significantly the stresses in the constant stress sectors of the un-constrained mode I fields and the mixed mode I/II fields can only differ by a hydrostatic term which depends in one case on the constraint as quantified by T/Q, and in the other on the level of mode mixity. On this basis it is possible to match the stresses in the leading sectors of mode I and mixed-mode fields. The implication of such a relationship is that for stress controlled cleavage failure the toughness of mixed mode I/II fields can be correlated with

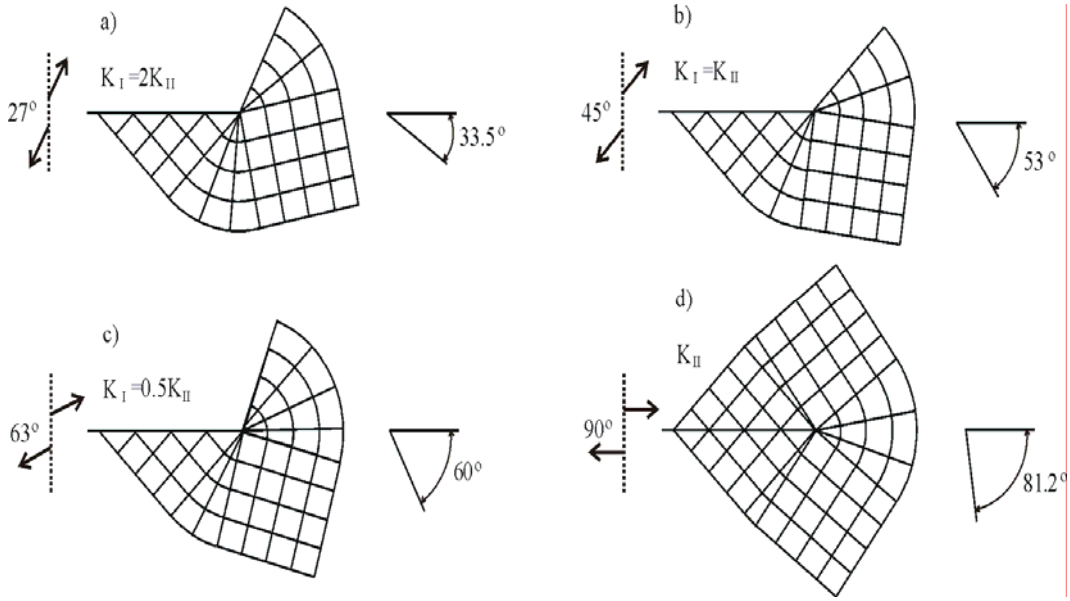

FIGURE 2. Slip line fields for a family of mixed-mode I/II problems at T=0.

those of unconstrained mode I configurations. In the present work this argument is developed for a strain hardening response and verified experimentally by fracture toughness experiments in mixed-mode loading and in unconstrained mode I fields.

Numerical method

Near tip fields have been examined under contained yielding conditions using the boundary layer formulation technique developed by Rice and Tracey [11], as modified to incorporate T-effects. The near tip region was modelled with a circular domain, to which the displacements corresponding to the first two terms in the Williams [12] expansion were applied as boundary conditions. Contained yielding develops close to the crack tip, while the remote field remains elastic representing contained yielding conditions. Mixed-mode fields were examined for four levels of remote mixity, defined by the ratio of Mode I stress intensity factor to Mode II stress intensity factor:

$$M^e = \frac{2}{\pi}\tan^{-1}\left(\frac{K_I}{K_{II}}\right) \tag{2}$$

The levels of mixity shown in Figure 3 were applied as displacements to the outer radius of the boundary of the finite element mesh, to the neglect of higher order terms. The mesh comprised 576 second order quadrilateral elements implemented in ABAQUS [13] and focused at the crack tip. The crack tip was represented by twenty four collapsed quadrilaterals such that the crack tip comprised 48 coincident but independent nodes. Calculations were performed for a strain hardening material, where the material response was represented by a Ramberg-Osgood relation with strain hardening exponents of 12 and 6 under both mode I and mixed-mode I/II conditions. Using a cylindrical co-ordinate system (r,θ) centred at the crack tip, plots of maximum hoop stress, $\sigma_{\theta\theta}$, are given as a function or radial distance from crack tip in Figure 3. The stresses are normalised by the yield stress, σ_o, while the radial distance from the crack tip normalised by J/σ_o. The stress profiles in the unconstrained Mode I and mixed-mode fields are similar on the plane of maximum hoop stress and comparison of the deviatoric stress profiles shows that the fields differ only by a hydrostatic term (Li [14], Bezensek [15]) under both strain hardening and perfectly-plastic conditions.

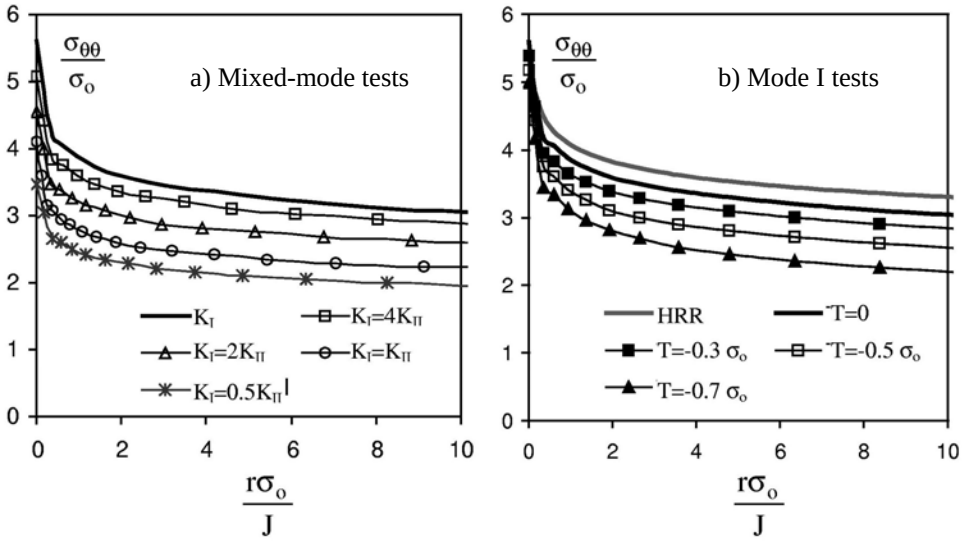

FIGURE 3. The maximum hoop stress for unconstrained mode I and mixed-mode cracks as a function of the non-dimensionalised distance from the crack tip; n=12.

Experimental

Specimens of width, W=24 mm, thickness, B=11.5 mm and length 130 mm were machined from bars of a plain carbon steel (BS En32) whose chemical composition is given in Table 1. Tensile tests have characterised the material with 0.2% yield stress of 430 MPa at -90 ^{o}C, and a strain hardening coefficient of 9. Young's modulus, E, was measured to be 217 GPa and Poisson's ratio, ν, was taken to be 0.3. Fracture mechanics specimens were pre-notched with a slitting wheel and fatigue pre-cracked to an a/W ratio of 0.5, in accordance with ASTM E399-88 [16]. Shallow cracked bend bars were obtained by machining the deeply cracked specimens, while maintaining the width of the uncracked ligament. Tests were performed using an environmental chamber cooled with liquid nitrogen at -90 ^{o}C. Temperature was measured with spot-welded thermocouples and was maintained within ±2 ^{o}C during testing. Before applying the displacement controlled load at cross-head velocity of 0.5 mm/min, specimens were maintained at the test temperature for a minimum of 12 minutes.

C	Si	Mn	P	S	Cr	Mo	V
0.18	0.26	0.70	0.014	0.027	0.10	0.02	<0.003

TABLE 1. Chemical composition of En32 steel (in wt%)

Mode I tests were performed on deep (a/W=0.5) and shallow (a/W<0.3) edge cracked bend bars in symmetric three-point-bending (3PB). Mixed-mode tests were performed in asymmetric four-point-bending configuration described by Maccagno and Knott [17], which allows the use of the same type of specimens and provides a wide range of mode mixities, by positioning the specimen in a stress field with combined shear and bending components. Crack propagation occurred at angle close to the plane of maximum principal stress allowing the crack to extend in a locally in mode I [18,19]. Fracture toughness was quantified by critical values of the J-integral which was decomposed into elastic and plastic components:

$$J_{el} = (K_I^2 + K_{II}^2)/E' \tag{3}$$

where E'=E/(1-ν^2) for plane strain. The mode I and mode II stress intensity factors were calculated using expressions given by Maccagno and Knott [17]:

$$K_I = \frac{M}{BW^{3/2}} Y_I, \quad K_{II} = \frac{Q}{BW^{1/2}} Y_{II}, \tag{4}$$

The plastic component of J was determined from the plastic work under load – crack-mouth-opening-displacement record:

$$J_{pl} = \frac{\eta_{CMOD}}{B(W-a)} A_{pl}^{CMOD} \tag{5}$$

The appropriate η_{CMOD} factors for mode I have been tabulated by Kirk and Dodds [20] for shallow mode I cracks. For mixed-mode I/II loadings specific η_{CMOD} factors were calculated using finite element model for each test configurations as discussed in detail by Bezensek [15]. The fracture toughness was then expressed in stress intensity factor notation as:

$$K_{Jc} = \sqrt{(J_{el} + J_{pl})/E'} \tag{6}$$

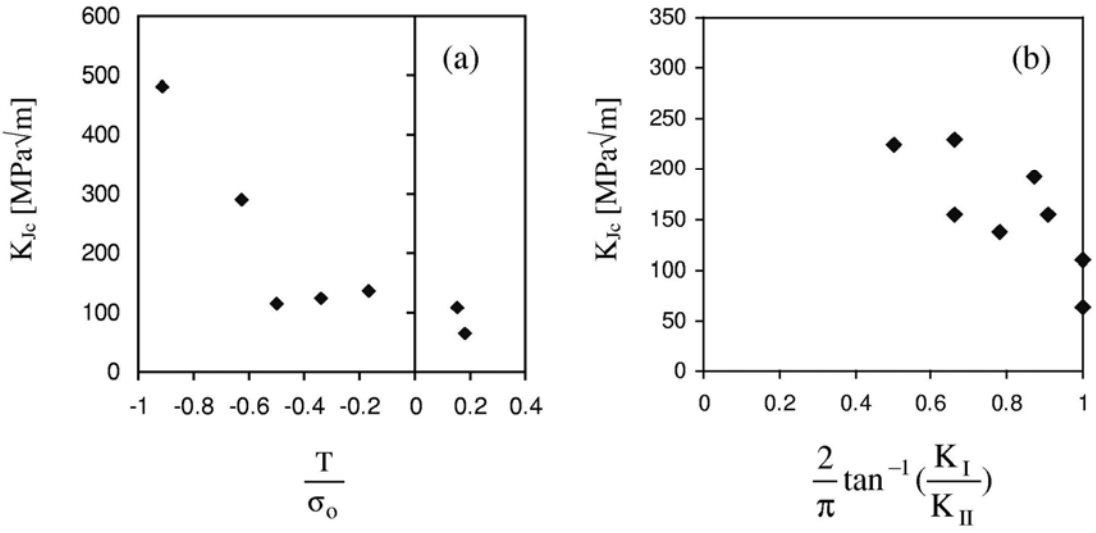

FIGURE 4. Results of fracture toughness tests: a) unconstrained Mode I test and b) mixed-mode I/II tests.

Failure occurred by cleavage in large scale plasticity, although minor ductile tearing occurred before cleavage in the most highly unconstrained fields which are a feature of very shallow mode I cracks (a/W<0.1) and highly mixed mode fields (M^e<0.66). The extent of ductile tearing was, in all cases, less than 0.3mm. In mode I, shallow cracked bend bars showed enhanced levels of toughness compared to deeply cracked bars, due to constraint. In mixed mode loading the toughness level increased with mixity as shown by the fracture toughness values in Figure 4. The data are analysed in Figure 5 using failure assessment diagrams of R6/4 [21], which are used to infer margins against failure by interpolating between elastic fracture and plastic collapse modes of failure of a cracked structure. For mixed-mode loading, the R6 recommends the use of the effective stress intensity factor, defined by superposition of mode I and mode II contributions, while the relevant failure assessment curves are at present those for the mode I data. The loads are normalised by the

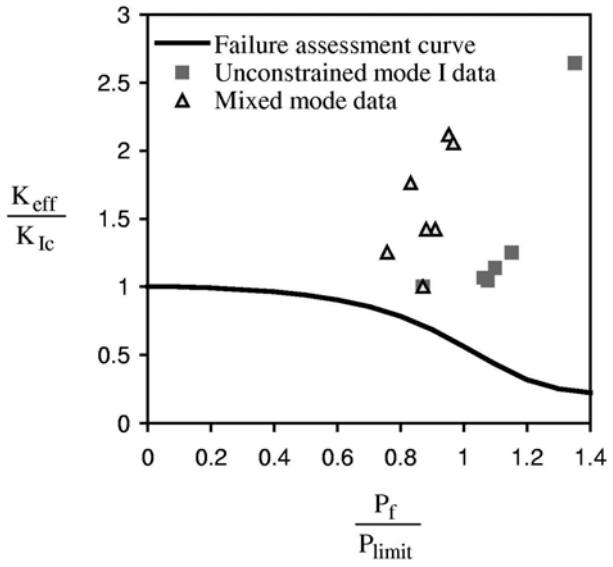

FIGURE 5. Unconstrained Mode I and mixed-mode I/II toughness data plotted in a failure assessment diagram.

limit load of each configuration, obtained from a full-field solution using ABAQUS, while K_{eff} on the ordinate is normalised with the lower bound deep cracked mode I value [21]. In this manner both sets of results are assessed independently. The results of unconstrained mode I and mixed-mode tests are consistent as shown in Figure 5. The data are conservative with respect to the general failure assessment line. This conservatism can be reduced by using a Constraint Modified Failure Assessment Diagram approach as discussed by Ainsworth and O'Dowd [22] and MacLennan and Hancock [23].

Discussion

It is frequently argued that the direction of crack extension in mixed-mode failure under brittle conditions occurs at the orientation at which the propagating crack extends in Mode I, or on the plane of maximum hoop stress [18,19]. In perfectly-plastic materials maximum hoop stress is the direction radially out through the apex of the constant stress diamond. At this angle the maximum hoop stress in mixed-mode fields may be compared with the stress in an unconstrained mode I field. The two fields can then be matched by relating constraint, T/Q, with mixity, M^e at a local fracture stress. This approach has also been shown to apply for strain hardening materials, and establishes a relationship between mixity and constraint shown in Figure 6.

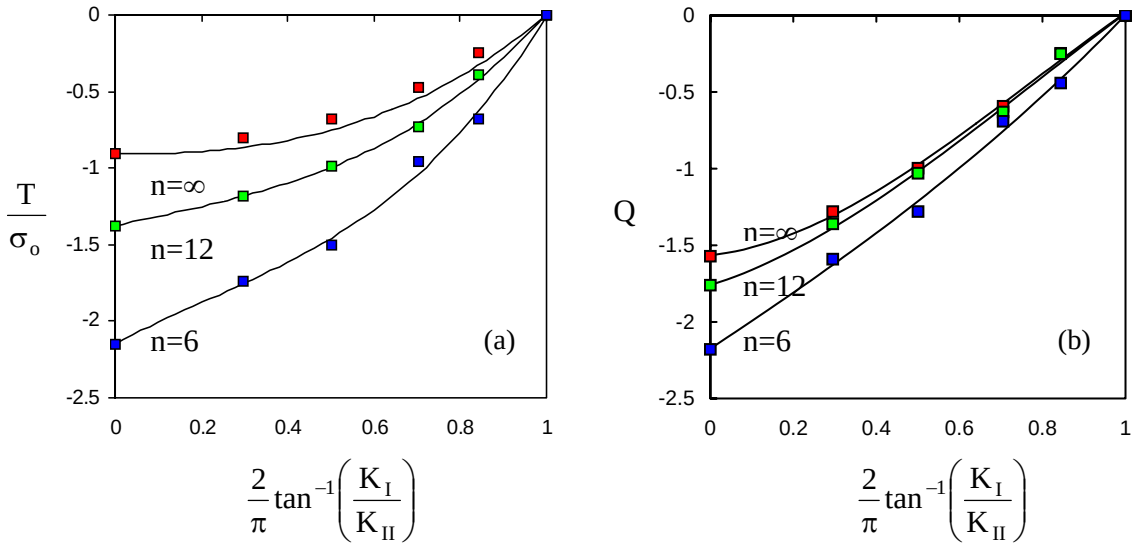

FIGURE 6. T-stress in (a) and Q in (b) as a function of elastic mixity for a range of strain hardening rates, obtained by matching fields at a local fracture stress and a non-dimensional distance of $2J/\sigma_o$.

In the leading sectors around the plane of maximum hoop stress, mixed mode field can be interpreted as belonging to the same family as mode I fields. Constraint loss by mixed-mode loading results in a family of fields which differ largely hydrostatically on the plane of maximum hoop stress and have a similar structure to those in mode I. For stress controlled brittle fracture this allows the constraint enhanced toughness observed in unconstrained Mode I fields to be correlated with the constraint enhanced toughness in mixed-mode loading, as shown with the failure locus in Figure 7.

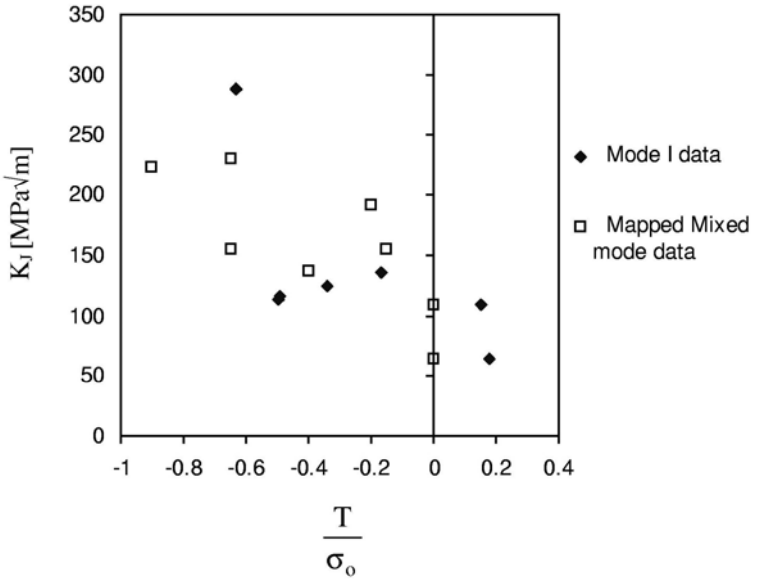

FIGURE 7. Unification of mode-mixity and in-plane constraint loss, shown by Mode I data and mapped mixed mode I/II data into a common constraint-mixity locus.

Acknowledgements

Authors are pleased to acknowledge access to ABAQUS under academic licence from Hibbitt, Karlsson and Sorensen. B. Bezensek is grateful to the Ministry of Science, Sport and Education of Slovenia for financial support and the Faculty of Mechanical Engineering, University of Maribor, Slovenia, for granting leave of absence to complete this work at the University of Glasgow. The authors are pleased to acknowledge the contributions of Dr. A. D. Karstensen and Dr. J. Li.

References

1. Smith, M.C., *The application of R6 appendix 7 to mixed-mode fracture test of a pressure vessel steel,* Report E/REP/GEN/0022/00, British Energy Generation Ltd, UK, 2000
2. Betegon C. and Hancock J.W., *J. Appl. Mech*, vol. **58**, 104-110, 1991
3. O'Dowd, N.P. and Shih, C.F., *J. Mech. Phys. Solids*, Vol. **39**, 939-963, 1991
4. Prandtl, L., *Nachr. Ges. Wiss*, 74-85, 1920
5. Du, Z.Z. and Hancock, J.W., *J. Mech. Phys. Solids*,, Vol. **39**, 555-567, 1991
6. Karstensen, A., *Constraint Estimation Schemes in Fracture mechanics.* PhD thesis University of Glasgow, UK, 1996
7. Li, J. and Hancock, J.W., *Int. J. Solids and Structures*, vol. **36**, 711-725, 1999
8. Shih, C.F., *ASTM STP 560*, ASTM Philadelphia, Pa, 187-210, 1974
9. Hutchinson, J.W., *J. Mech. Phys. Solids*, Vol. **16**, 13-31, 1968
10. Zhu, X.K. and Chao, Y.J., *J. Mech. Phys. Solids*, vol. **40**, 511-536, 2001

11. Rice, J.R. and Tracey, D.M., In: *Numerical and computational methods in structural mechanics*, Academic Press, New York, 1973

12. Williams, M.L., *ASME J. Applied Mechanics*, vol. **24**, 111-114, 1957

13. ABAQUS/Standard V5.8, Hibbit, Carlsson and Sorrensen, Providence, Rhoad Island, Pa

14. Li, J., *Elastic-plastic interfacial crack problems*, PhD Thesis, University of Glasgow, UK, 1997

15. Bezensek, B., *Elastic-plastic crack problems in the ductile-brittle transition*, PhD Thesis, University of Glasgow, UK, 2003

16. ASTM E399, *Standard method for plane strain fracture toughness testing of metallic metals*, Vol. **03.01**, American Society for Testing and Materials, Philadelphia, 1988

17. Maccagno, T.M., and Knott, J.F., *Eng. Fract. Mech.*, Vol. **34**, 65-86, 1989

18. Erdogan, F., and Sih, G.C., *J. Basic Eng*, Vol. **85**, p.519, 1963

19. Williams, M.L. and Ewing, P.D. *Int. J. Fracture Mechanics*, vol. **8**, p.441, 1972

20. Kirk, M.T., and Dodds, R.H., *J. Testing Eval.*, Vol. **21**, 228-238, 1993

21. R6, *Assessment of the integrity of structures containing defects*, Revision 4, British Energy Generation Ltd, Gloucester, UK, 2001

22. Ainsworth, R.A. and O'Dowd, N.P., *Int. J. Pressure Vessels and Piping*, vol. **117**, 260-267, 1995

23. MacLennan, I.J. and Hancock, J.W., In: *Proc. Roy. Soc. London Series A*, vol. **451**, 757-777, 1995